Cerebral Cortex April 2012;22:820–827
doi:10.1093/cercor/bhr148
Advance Access publication June 21, 2011

Spatial and Temporal Bias in the Mitotic Origins of Somatostatin- and Parvalbumin-Expressing Interneuron Subgroups and the Chandelier Subtype in the Medial Ganglionic Eminence

Melis Inan, Jelle Welagen and Stewart A. Anderson

Department of Psychiatry, Weill Medical College of Cornell University, New York, NY 10021, USA

Melis Inan and Jelle Welagen contributed equally to this work

Address correspondence to Dr Stewart A. Anderson, Weill Medical College of Cornell University, 1300 York Avenue, Box 244, New York, NY 10021, USA. Email: saa2007@med.cornell.edu.

GABAergic interneurons modulate cortical activity through the actions of distinct subgroups. Recent studies using interneuron transplants have shown tremendous promise as cell-based therapies for seizure disorders, Parkinson's disease, and in the study of neocortical plasticity. Previous reports identified a spatial bias for the origins of parvalbumin (PV)- and somatostatin (SST)-expressing interneuron subgroups within the medial ganglionic eminence (MGE). In the current study, the mitotic origins of these interneurons are examined by harvesting MGE cells at 2 time points and evaluating their neurochemical profiles after transplantation into neonatal mouse cortex. Although the dorsal MGE (dMGE)-SST and ventral MGE (vMGE)-PV bias were confirmed, both subgroups originate from progenitors located throughout the MGE. The dMGE bias was also found for SST subgroups that coexpress calretinin or reelin. In contrast, another major subgroup of SST interneuron, neuropeptide Y-expressing, does not appear to originate within the MGE. Finally, novel evidence is provided that a clinically important subtype of PV-expressing interneuron, the chandelier (axo-axonic) cell, is greatly enriched in transplants from the vMGE at embryonic day 15. These findings have important implications both for the study of interneuron fate determination and for studies that use interneuron precursor transplantation to alter cortical activity.

Keywords: chandelier, interneuron, medial ganglionic eminence, parvalbumin, somatostatin.

Introduction

Different classes of neurons in the mammalian central nervous system (CNS) are generated by induction of a transcriptional code in neuronal progenitors, which is regulated by activation of cell–cell interaction as well as morphogen-dependent signaling cascades (Lee and Pfaff 2001; Malicki 2004). Two well-characterized structures within the CNS are the spinal cord (Lee and Pfaff 2001) and the retina (Malicki 2004) where progenitors are restricted to distinct fates spatially and temporally, respectively.

With its neuronal heterogeneity, the mammalian neocortex is one of the most challenging regions to study the mechanisms involved in the generation of neuronal diversity. Much of this heterogeneity arises from γ-aminobutyric acidergic interneurons, which comprise diverse populations that are subclassified based on morphology, intrinsic physiology, neurochemical markers, and axon targets (Markram et al. 2004; Ascoli et al. 2008). Fate-mapping studies have demonstrated the presence of spatially and temporally distinct progenitor domains for interneuron subclasses within the embryonic ventral (subcortical, pallidal) telencephalon (for recent reviews, see Batista-Brito and Fishell 2009; Gelman and Marin 2010; Welagen and Anderson 2011).

Most neocortical interneurons, including all or nearly all of 2 major nonoverlapping subgroups defined by their expression of parvalbumin (PV) or somatostatin (SST), originate in the medial ganglionic eminence (MGE) (Wonders and Anderson 2006). Transplantation and genetic fate-mapping studies have demonstrated that there is a bias for the generation of SST-expressing interneurons (SST^+) from the dorsal MGE (dMGE), whereas PV-expressing interneurons (PV^+) tend to be generated from ventral regions (vMGE) (Flames et al. 2007; Fogarty et al. 2007; Wonders et al. 2008). This bias appears to relate to enhanced Shh signaling within the dMGE Xu, Guo, et al. (2010). However, only one of these studies specifically examined the mitotic origins of these interneuron subgroups, finding that SST^+ interneurons, labeled at the progenitor stage with the S-phase marker BrdU and examined after 10 days of culture, can originate from both d- and vMGE (Wonders et al. 2008).

Better defining the mitotic origins of cortical interneurons is important for 2 reasons. First, understanding the link between intra-MGE patterning and mitotic origins of interneurons is a critical step to discovering the mechanisms giving rise to interneuron subtype diversity. Second, MGE transplants into postnatal cortex have been shown to enhance local inhibition (Alvarez-Dolado et al. 2006), alter cortical plasticity (Southwell et al. 2010), and offer remarkable promise as a cell-based therapy for seizures (Baraban et al. 2009; Waldau et al. 2010; Zipancic et al. 2010) as well as Parkinson's disease (Martinez-Cerdeno et al. 2010). Since the PV- and SST-expressing subgroups have distinct intrinsic firing properties and distinct propensities for targeting the perisomatic versus distal dendritic regions of pyramidal neurons (Markram et al. 2004), better understanding of interneuron subgroup compositions from temporally and spatially defined MGE sources will critically inform future transplantation studies.

In this paper, pan-green fluorescent protein (GFP) expressing mouse dams were injected with BrdU at E13.5 or E15.5 to label cells in S-phase. Two hours later, the dorsal (d), middle (m), or ventral (v) regions of the MGE were transplanted into neonatal neocortex, and the fates of transplanted cells were evaluated after 30 days. Although we confirmed the bias for SST^+ interneurons to be dMGE-derived, and PV^+ interneurons to originate within vMGE, a surprising number of both subgroups were generated from mitosis in the opposite region. In addition, analysis of interneuron morphology by GFP immunolabeling resulted in the novel finding that a functionally and clinically relevant subclass of PV^+ interneuron, the

chandelier (axo-axonic) cell, is greatly enriched within the vMGE transplants at E15.5.

Materials and Methods

In Vivo Transplantation

For in vivo labeling of S-phase donor cells, pregnant females were injected intraperitoneally with BrdU (100 mg/kg) 2 h prior to their sacrifice by an overdose of sodium pentobarbitol and thoracotomy. The day of vaginal plug was considered embryonic day 0.5 (E0.5). GFP$^+$ brains of E13.5 and E15.5 embryos were sectioned in the coronal plane, 250 μm thick, using a vibrating microtome (Thermo Scientific HM650V). Slabs of tissue corresponding to the dorsal, middle, and vMGE regions were dissected using fine forceps (Fig. 1). Although some mantle zone was likely to be present in each dissection, an effort was made to limit dissections mainly to the proliferative zones using the increased opacity of this region. To limit the rostral–caudal level of the dissections, these were made only where the MGE–lateral ganglionic eminence (LGE) sulcus is evident and no thalamus is present in the dorsal midline. Samples obtained from both hemispheres of 2 slices from 2 embryos were combined and considered as an individual experiment for statistical purposes. Donor cells were dissociated by trituration, centrifuged at 500 g for 5 min, resuspended in 15–30 μL of NB/B27 medium and adjusted to a cell concentration of roughly 40 cells/nL. The cells were suction filled into a beveled glass micropipette (0.5 mm inner diameter, 1 mm outer diameter), fitted to an oocyte nanoinjector (Nanoinject II, Drummond), and injected into cooling-anesthetized neonatal (P0–P2) pups. The use of this injector allowed for the minimization of tissue damage by injecting small volumes at a relatively slow rate (23 nL/s). Each pup received 35 injections of 69 nL into each hemisphere placed 1 mm lateral to the midline and 1 mm rostral to the interaural line, targeting somatosensory cortex. The micropipette tip was placed 1 mm deep to the pial surface, allowing for the injection of cells mainly into layers 3, 4, and 5.

Tissue Collection and Immunofluorescence Labeling

Pups that received cell injections were sacrificed at P30. The mice were perfused intracardially with 1× phosphate-buffered saline (PBS) followed by 4% paraformaldehyde (PFA) and postfixed in fresh 4% PFA for 4 h. The brains were then removed and sectioned in the coronal plane at 40 μm on a vibrating microtome. Primary antibodies used for immunofluorescence labeling included mouse anti-BrdU (1:400; Chemicon), chicken anti-GFP (1:2000; Molecular Probes), rabbit anti-PV (1:5000; Swant), rat anti-SST (1:400; Chemicon), rabbit anti-CR (1:1000; Milipore), rabbit anti-NPY (1:1000; Immunostar) and mouse anti-Rln (1:1000; kindly provided by Andre M. Goffinet). Fluorescent secondary antibodies were Alexa 488 and 568 (1:500; Molecular Probes) and Cy5-conjugated (1:500; Jackson Immunoresearch). The nuclear marker DAPI (300 nM) was applied together with the secondary antibodies.

Sections were first processed with primary antibodies for SST or PV and GFP followed by their corresponding secondary immunolabeling. The slices were then fixed in 4% PFA for 30 min and processed for BrdU immunostaining by incubation in 2 N HCl in PBS at 37 °C for 15 min and then 0.1 M boric acid for 2 min. Then they were rinsed, blocked in 5% fetal calf serum, and treated overnight with mouse anti-BrdU (1:400; Chemicon). The next day, the slices were treated with secondary antibodies for BrdU (1:500; Alexa 568 goat anti-mouse; Molecular Probes). The signal was detected by epifluorescence microscopy (Nikon) using a 40× objective and images acquired using a cooled CCD camera (Coolsnap HQ, Roper; Metamorph software, Universal Imaging). Epifluorescence microscopy was appropriate for this quantification since the low density of labeling renders the perfect superimposition of labeled cells a very rare event (see examples in Fig. 2; we have previously confirmed that confocal microscopy of labeled cells in similar transplants results in equivalent results but at a far higher cost and limits the ability to reexamine the material due to photobleaching).

Data Collection and Analysis

Cell profile counts were made in the somatosensory cortex between the genu of the corpus callosum and the hippocampal commissure. Statistical comparison between dMGE, mMGE, and vMGE samples was performed using unpaired one-way analysis of variance (ANOVA) combined with a post hoc Tukey's, unless otherwise stated.

Results

To examine the relationship between mitotic origin within the MGE and interneuron subgroup fate, pan-GFP-expressing males were crossed to wild-type females, and a single BrdU pulse (100 mg/kg; intraperitoneally) was injected into the dam 2 h before euthanization of the dam and dissection of the GFP$^+$ embryos. The dMGE, mMGE, vMGE subregions were removed from embryos at embryonic day 13.5 (E13.5) and E15.5, dissociated, and transplanted into the cortex of P0–P2 hosts (Fig. 1*A*–*C*). Colabeling of BrdU and GFP with interneuron subgroup markers PV or SST was

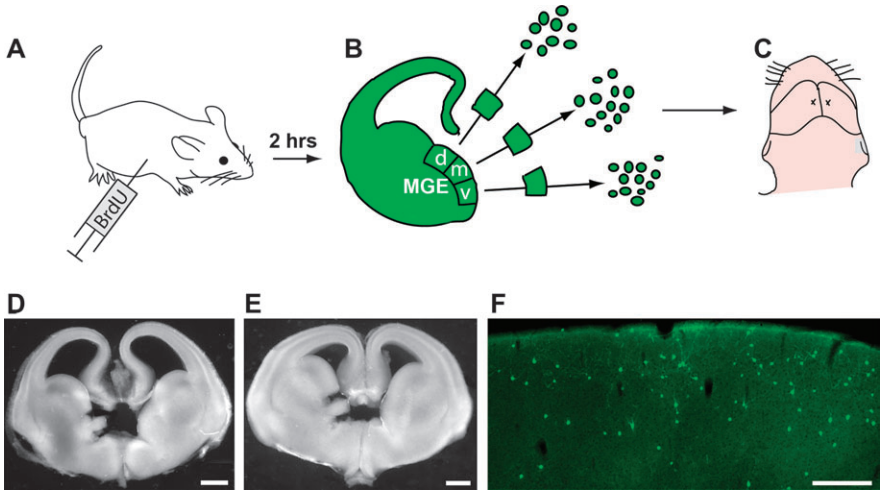

Figure 1. Experimental design. (*A*) Two hours before euthanization, BrdU (100 mg/kg; intraperitoneally) was injected into the dam carrying pan-GFP expressing pups at E13.5 or E15.5. (*B*, *C*) Brains were sectioned on a vibrating microtome, and the dorsal (d), middle (m), or ventral (v) subregions of the MGE were dissociated and transplanted into the cortex of neonatal hosts (*C*). (*D*, *E*) Examples of coronal slices from which d- and vMGE were dissected at E13.5 (*D*) and E15.5 (*E*). (*F*) Immunofluorescence labeling of GFP-expressing cells at postnatal day 30 neocortex. Scale bars: 200 μm.

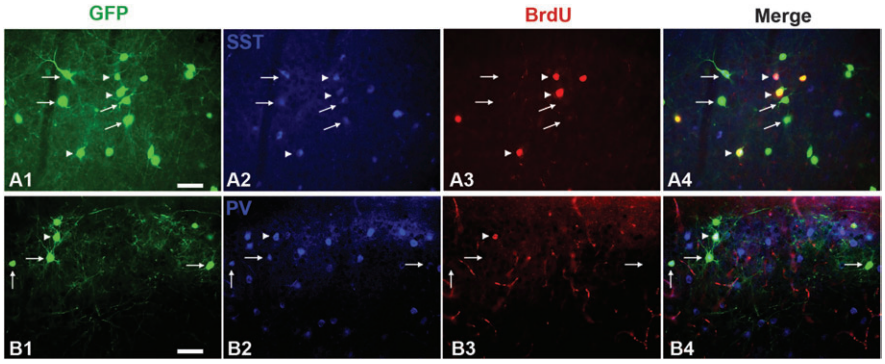

Figure 2. BrdU and GFP colabeling with PV or SST in MGE transplants. MGE-derived GFP$^+$ cells transplanted into the neocortex (A1, B1) give rise to SST-expressing (A2, A4) and PV-expressing (B2, B4) interneurons. GFP$^+$ cells that originate from progenitors in S-phase (arrowheads) at the time of transplant colabel with BrdU (A1, 3, 4, B1, 3, 4). BrdU staining is absent in GFP$^+$ cells that were not in S-phase at the time of transplant (arrows). Scale bars: 50 μm.

then quantified in sections through the somatosensory cortex of mice at P30 (Fig. 2). In these transplants, cells were plentiful within roughly 1 mm from the injection site (Figs 1*F* and 2), consistent with previous studies using neonatal neocortical transplantation of MGE-derived cells (Cobos et al. 2005; Alvarez-Dolado et al. 2006; Du et al. 2008; Wonders et al. 2008; Baraban et al. 2009).

First, the percentage of GFP$^+$ cells transplanted from different regions of the MGE at E13.5 and E15.5 that colabeled with BrdU were analyzed. There was no significant difference between different regions at both of the ages tested (%BrdU$^+$, GFP$^+$ [±standard error of the mean, SEM], n = 3: E13.5 dMGE: 10.5 ± 5.0, mMGE: 12.3 ± 4.9, vMGE: 6.2 ± 2.6 and for E15.5: 10.5 ± 2.0, 10.1 ± 0.8, 10.5 ± 1.1, $P > 0.05$). Since essentially all BrdU$^+$ cells colabel with GFP, BrdU$^+$ and GFP$^+$ colabeled neurons are referred to simply as "BrdU$^+$."

SST$^+$ and PV$^+$ Interneuron Subgroups Originate Throughout the MGE with an Opposing Bias on the Dorsal–Ventral Axis

At E13.5, quantification of SST$^+$, BrdU$^+$ colabeled cells within BrdU$^+$ neurons (SST$^+$/BrdU$^+$) revealed a dMGE-high and vMGE-low spatial gradient (Fig. 3; % SST$^+$/BrdU$^+$ (±SEM), n = 3: dMGE: 45.3 ± 2.9, mMGE: 28.0 ± 3.1, vMGE: 8.7 ± 1.3, (dMGE vs. mMGE: $P < 0.01$, dMGE vs. vMGE: $P < 0.001$, mMGE vs. vMGE: $P < 0.01$)). Counts of PV$^+$/BrdU$^+$ neurons revealed an opposite gradient, although dMGE transplants still contained a substantial percentage of PV$^+$ interneurons (Figs 2 and 3; % PV$^+$/BrdU$^+$ [±SEM], n = 3: dMGE: 29.1 ± 3.5, mMGE: 29.4 ± 10.3, vMGE: 51.5 ± 3.6; vMGE vs. dMGE: one-way ANOVA with post hoc Tukey's $P < 0.06$, NS, but by t-test vMGE vs. dMGE $P < 0.01$).

Comparison of the percentage of cells labeled with BrdU versus all GFP$^+$ cells revealed similar results for both SST and PV at E13.5 (Fig. 3). The transplanted GFP population is mixed with a component of S-phase cells (about 10%, see above), cycling cells that were not in S-phase during the BrdU pulse (probably no more than triple the % of BrdU$^+$ cells), as well as postmitotic cells that could either have been from the same or from a different mitotic origin. Thus, the similar results in counts of colabeling with BrdU or GFP suggest that the transplanted regions do not contain a large component of cells that originated from outside of the dissected region at this age.

In marked contrast to the results from E13.5 transplants, in E15.5 transplants, a low percentage of BrdU$^+$ cells expressed SST regardless of the MGE region used. In addition, there was

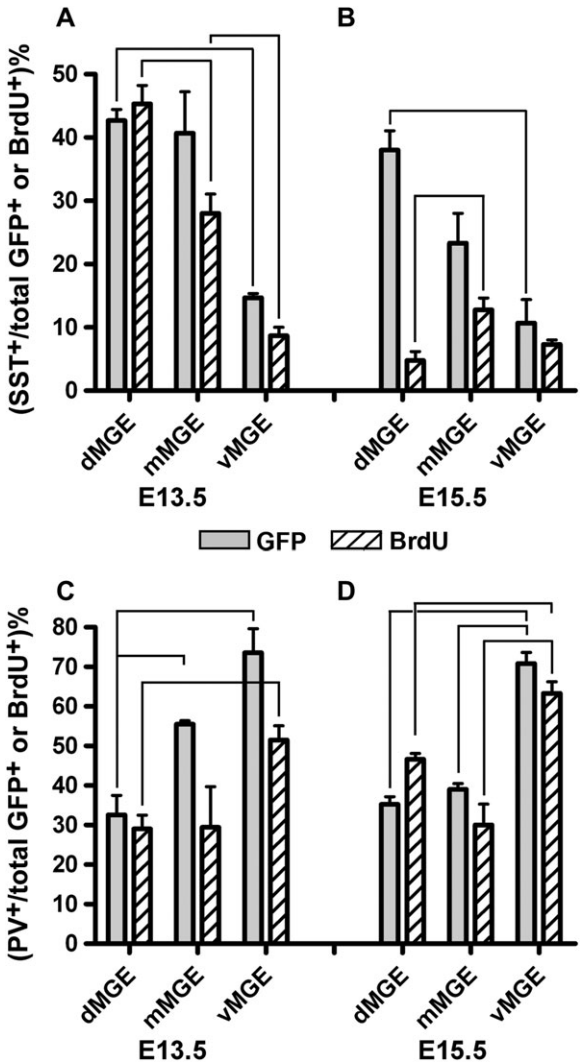

Figure 3. Quantification of regional and temporal differences in transplanted MGE cells expressing SST or PV. Bars represent percentages of either GFP$^+$ cells (solid pattern) or BrdU$^+$ cells (striped pattern) that colabel for SST (*A*, *B*) or PV (*C*, *D*) at E13.5 (*A*, *C*) and E15.5 (*B*, *D*). Lines connecting bars indicate significant differences with $P < 0.05$ (generally unpaired one-way ANOVA, post hoc Tukey; see Materials and Methods for details on statistical analysis).

no bias for dMGE to generate more of these cells than mMGE or vMGE (Fig. 3; % $SST^+/BrdU^+$ ±SEM, $n = 3$: dMGE: 4.8 ± 1.4, mMGE: 12.8 ± 1.9, vMGE: 7.3 ± 0.7; dMGE vs. mMGE, $P < 0.05$). Surprisingly, at E15.5, the dMGE high vMGE low gradient of SST expression by all GFP^+ cells remained (Fig. 3; E15.5, dMGE: 38.0 ± 3.1, mMGE: 23.3 ± 4.7, vMGE: 10.7 ± 3.7; dMGE vs. vMGE, $P < 0.01$).

The finding that almost 40% of transplanted dMGE cells (GFP^+) express SST, but only 5% of dMGE cells that are $BrdU^+$ express SST indicates that most cells in the dMGE that go on to express SST are already postmitotic at E15.5. (E15.5 dMGE SST^+ GFP^+ vs. $BrdU^+$: $P < 0.0006$, $n = 3$, t-test). Since transplants from mMGE and vMGE also give rise to low percentages of SST^+ cells, this result also suggests that many of the SST-committed precursors remain in the dMGE after cell cycle exit before migrating to the cortex.

Similar to the results with SST colabeling with BrdU, the vMGE bias for origin of PV interneurons was less pronounced at E15.5 than at E13.5 but remained statistically significant (% $PV^+/BrdU^+$ [±SEM], $n = 3$: dMGE: 46.7 ± 1.4, mMGE: 30.0 ± 5.3, vMGE: 63.3 ± 2.9; dMGE vs. mMGE and dMGE vs. vMGE: $P < 0.05$, mMGE vs. vMGE: $P < 0.01$, Fig. 3). There was a strong tendency for transplants at E15.5 to give rise to more PV than SST interneurons compared with the transplants at E13.5. This result is consistent with the generally "inside-out" gradient of neurogenesis for PV- and for SST-expressing interneurons in the neocortex (Cavanagh and Parnavelas 1988; Rymar and Sadikot 2007; Wonders et al. 2008) and with the far greater relative density of PV versus SST interneurons in superficial versus deep neocortical layers (Xu et al. 2010).

E15.5 vMGE Transplants Are Highly Enriched for Chandelier Interneurons

The results presented above strongly support a model whereby PV and SST interneurons are generated, at least for the most part, by progenitors that are differentially biased to be located in the ventral or dorsal portions of the MGE, respectively (Fig. 3). At the same time, overlap exists in the PV- or SST-producing domains. This raises the question of whether subtypes of interneurons (defined by combinations of neurochemical, electrophysiological, and morphological-/axon-targeting characteristics) within these neurochemically defined subclasses may have subdomains of generation within the MGE.

To address this question, we focused on "fast-spiking," PV-expressing interneurons that contain 2 main subclasses, basket, and chandelier cells (Ascoli et al. 2008). PV^+ basket cells tend to have curved axonal terminals that mainly target pyramidal neuron somata and proximal dendrites. In contrast, the far more rare PV^+ chandelier interneurons (also known as axo-axonic cells) have vertically oriented terminals (cartridges) that target the axon initial segment of pyramidal neurons (Somogyi 1977; Somogyi et al. 1982; DeFelipe et al. 1985). Genetic fate-mapping studies have previously identified the MGE as the likely source of chandelier interneurons (Xu et al. 2008; Fazzari et al. 2010). However, a more precise spatial or temporal source of these interneurons, dysfunction of which has been implicated in some forms of epilepsy and schizophrenia (DeFelipe 1999; Volk and Lewis 2002), has not been established.

Transplants of dorsal, middle, or ventral MGE at E13.5 or E15.5 were evaluated for the presence of chandelier interneurons, the axon terminals of which were easily identifiable by immunofluorescence labeling (Fig. 4*A*; see Materials and Methods). At E13.5, only about 3% of GFP^+ cells from the dMGE or mMGE transplants developed into chandelier interneurons (Fig. 4*B*). This value jumped to 10% in the vMGE. By comparison to the GFP^+/PV^+ colabeling data in Figure 3*C*, the results suggest that chandelier interneurons comprise less than 10% of the PV^+ interneurons in the 13.5 transplants. At E15.5, similar results to the earlier transplants were found for dMGE and mMGE sources. In contrast, vMGE transplants at E15.5 resulted in over 25% of GFP^+ cells becoming chandelier interneurons (Fig. 4*B*). As similar numbers (about 70%; Fig. 3) of vMGE GFP^+ cells differentiate into PV-expressing interneurons at E13.5 as at E15.5, the ratio of chandelier interneurons within the PV population nearly triples for this source relative to the other 5 sources tested. In sum, these results indicate that the vMGE at E15.5 is a major source of the chandelier subtype of PV-expressing interneuron (Fig. 6).

Origins of $SST^†$ Cells that Coexpress Other Cortical Interneuron Markers

The SST-expressing subgroup of cortical interneurons include cells that colabel with calretinin (CR), reelin (Rln), and Neuropeptide Y (NPY) (Gonchar et al. 2007; Xu et al. 2010; Miyoshi et al. 2010). Analysis of the origins of these smaller classes within the SST^+ subgroup of cortical interneurons is of interest as a particular bias for a certain class would be consistent with a distinct transcriptional code for that class within the MGE. Therefore, we analyzed the MGE origins of SST^+ cortical interneurons that coexpress these other markers in cells transplanted from different areas of the MGE.

Approximately 30% of all GFP^+ cells derived from d- and mMGE transplants also expressed CR, whereas very few CR^+ cells were generated from vMGE, if any. (% CR^+, SST^+/GFP^+, $n = 3$: at E13.5: dMGE: 19.3 ± 2.6, mMGE: 7.7 ± 3.3, vMGE: 1.3 ± 0.8, (dMGE vs. vMGE: $P < 0.01$), at E15.5: dMGE: 21.6 ± 2.4, mMGE: 12.9 ± 4.0, vMGE: 1.8 ± 0.8; dMGE vs. vMGE: $P < 0.01$). Analysis of CR and SST colabeling revealed that only around 1% of transplanted cells from any region of the MGE that are CR^+ did not express SST. Therefore, within the SST^+ subgroup, CR coexpressing–transplanted cells revealed a dorsal-high, ventral-low bias (Fig. 5) that closely resembles the bias for the SST^+ subgroup as a whole (Fig. 3).

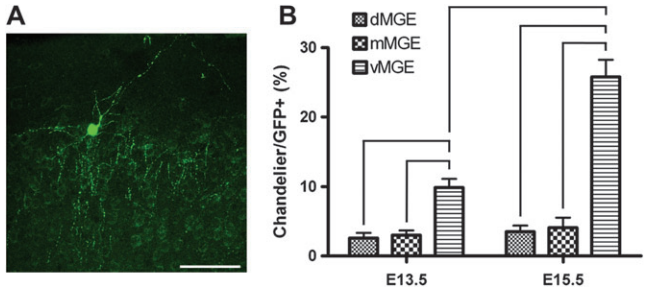

Figure 4. E15.5 vMGE transplants are highly enriched for chandelier interneurons. (*A*) Example of a transplanted cell with chandelier interneuron morphology. Note the prominent vertically oriented "cartridges" of axon terminals. (*B*) Quantification of transplanted cells with chandelier morphology. There was an enrichment of chandelier interneurons in the vMGE at both ages. At E15.5, this enrichment significantly increased relative to both dMGE and mMGE at E15.5 and relative to the vMGE in the E13.5 transplants. Bars above the graphs indicate significant differences using an unpaired one-way ANOVA, $P < 0.05$, post hoc Tukey. Scale bar: 100 μm.

Another marker that a subset of cortical and hippocampal SST^+ cells express is Rln (Pesold et al. 1998; Yabut et al. 2007; Miyoshi et al. 2010). However, in our samples about 95% of SST -expressing cells in somatosensory cortex colabeled with Rln, such that counts of Rln colabeling with GFP not surprisingly revealed a similar dMGE bias (% Rln^+/GFP^+, $n = 3$: dMGE: 66.2 ± 3.1, mMGE: 37.6 ± 8.0, vMGE: 12.0 ± 1.5; dMGE vs. vMGE: $P < 0.05$, dMGE vs. vMGE: $P < 0.001$, mMGE vs. vMGE: $P < 0.05$, Fig. 5).

Finally, analysis of the NPY^+ coexpression with GFP in MGE transplants revealed that very few NPY^+ cells are present in MGE transplants at E13.5 or E15.5 (less than 1% at E13.5 and no more than 3% at E15.5, Fig. 5). Of these, essentially all colabeled with SST, consistent with previous studies implicating the preoptic region or CGE as primary sources of these interneurons (Fogarty et al. 2007; Gelman et al. 2009).

Discussion

Previous studies found that a spatial bias for the origins of the 2 major neurochemically defined subgroups of cortical interneurons, those that express PV or SST, exists on the dorsal–ventral axis of the MGE (Flames et al. 2007; Fogarty et al. 2007; Wonders et al. 2008). Since particularly at later stages of neurogenesis, there is considerable, mainly dorsal-directed, migration within the proliferative zone of the MGE (Anderson et al. 2001), the current study extends these findings by focusing on the mitotic origins of these interneuron subgroups. Although the dMGE-SST vMGE-PV bias was confirmed, both PV and SST interneurons were found to derive from progenitors throughout the MGE. Additionally, a relatively rare but clinically relevant subtype of PV-expressing interneuron, the chandelier (axo-axonic) cell, was found to originate mainly within the most ventral region of the MGE with a significant enrichment at E15.5 compared with E13.5. These novel findings have important implications for the study of interneuron fate and for studies that use interneuron transplantation to alter cortical activity.

Like the spinal cord, the telencephalon is composed of molecularly distinct domains that give rise to distinct types of neurons. After E12.5, the MGE itself can be parsed into 5 molecular domains (Flames et al. 2007), the most dorsal of which strongly expresses Nkx6.2, a transcription factor associated mainly with progenitors of SST-expressing interneurons (Fogarty et al. 2007; Sousa et al. 2009). However, our results demonstrate that at E13.5, the mitotic origins of SST-expressing interneurons extend through the mid-region of the MGE (Fig. 3), well ventral to the detectable Nkx6.2 expression domain at this age. At the same time, while 40% of surviving $BrdU^+$ cells of the E13.5 dMGE gave rise to SST-expressing interneurons, some 30% of $BrdU^+$ cells in these transplants expressed PV. These results indicate that a substantial degree of mixing occurs in the mitotic origins of these neurochemically defined subgroups.

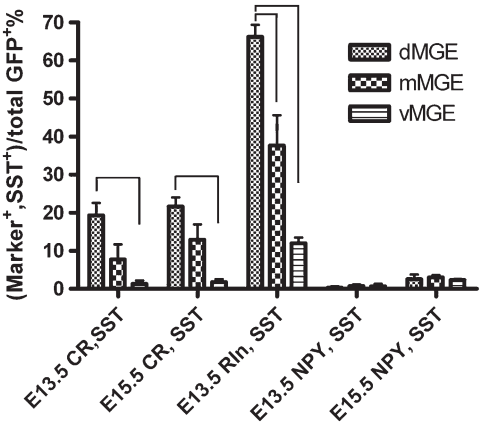

Figure 5. Quantification of regional and temporal differences in transplanted MGE cells coexpressing SST and either one of the SST subgroup markers calretinin (CR), reelin (Rln), or Neuropeptide Y (NPY). Bars represent percentages of GFP^+ cells derived from spatially and temporally distinct MGE regions. Lines connecting bars indicate significant differences with $P < 0.05$ (unpaired one-way ANOVA, post hoc Tukey; see Materials and Methods for details on statistical analysis).

Of note, in recent studies of a transgenic mouse line in which the Cre recombinase was inserted into the Shh locus, it was reported that the vMGE gives rise to few cortical interneurons, instead giving rise mainly to spiny PV^+ projection neurons of the globus pallidus as well as striatal interneurons (Flandin et al. 2010). However, we believe that much of the discrepancy with the current results is caused by different terminology for describing MGE subdomains. In the current paper, transplantations were carefully limited to the rostral–caudal level where both the MGE and LGE form large distinct structures but where the thalamus is not visible at the dorsal midline. In addition, at this more rostral level, the boundary between the vMGE and preoptic region is generally visible based on the presence of a small sulcus (Fig. 1*D*,*E*). At this level, Shh messenger RNA is not expressed in the proliferative zone. It is strongly expressed in the MGE mantle but without an apparent dorsal–ventral variation (see e.g., Fig. 2*O* in Gulacsi and Anderson (2008)). In Flandin et al. (2010), the regions showing Cre recombination appear to occur more caudally and occur prior to E13.5, the earlier of 2 time points used for MGE cell transplantation in the current study. In addition, at more caudal levels, the distinction between the MGE and underlying preoptic area (POA) is not obvious. In sum, one might refer to the results of the current paper pertaining to the rostral vMGE at peak times of cortical neurogenesis, whereas Flandin et al. focused on relatively early-born neurons from the caudal vMGE or possibly the most dorsal domain of the preoptic region. However, since we cannot differentiate between an aspiny PV^+ interneuron of the striatum or cortex (to our knowledge, a neurochemical or electrophysiological distinction in these interneurons has not been demonstrated), it is quite possible that our vMGE transplants contain some interneurons from mitoses that would have generated striatal rather than cortical interneurons. On the other hand, the selectively axon-targeting chandelier interneurons, which are quite plentiful in the vMGE transplants (almost 25%; Fig. 4), do not appear to exist in striatum.

The presence of mixed mitotic origins for PV- or SST-expressing subgroups within the MGE raises intriguing questions regarding interneuron fate determination. It was recently demonstrated that the dMGE domain, and SST fates that many of these progenitors attain, is specified by higher levels of Shh signaling (Xu et al. 2010). Lower levels of Shh are required to maintain Nkx2.1 expression and PV-expressing interneuron fate. The presence of mitotic origins of both PV- and SST-expressing interneurons within the dMGE suggests that mechanisms for the differential fate determination of these subgroups may be more complicated than the gradient of Shh

signaling that specifies relatively pure domains of neuronal fates in the ventral spinal cord (Jessell 2000). Notch signaling, perhaps by influencing the degree to which individual progenitors read out the Shh concentration, is one possibility for generating this diversity. Another possibility is that some radial progenitors of cortical interneurons are multipotential, generating mainly SST interneurons with apical neurogenic divisions, and PV interneurons from basal intermediate progenitor divisions (Glickstein et al. 2007).

Based on genetic temporally restricted fate mapping combined with electrophysiological and neurochemical characterization, it has been suggested that MGE progenitors progress from generating mainly SST to mainly PV interneurons (Miyoshi et al. 2007). This genetic labeling of relatively more SST-expressing interneurons and SST-correlated electrophysiological subclasses, earlier during the neurogenic period, and more PV^+ fast-spiking interneurons later, is consistent with the "inside-out" relationship of these subgroups' birthdate to laminar location (Cavanagh and Parnavelas 1988; Wonders et al. 2008) and with the far higher ratio of PV to SST interneurons present in superficial cortex of mice (Xu et al. 2010). The results of the current study also show that PV^+ interneurons make up a much higher percentage of the transplanted cells at E15.5 than E13.5, particularly from the dMGE (Fig. 3). However, a temporal progression of MGE interneuron production in favor of more PV^+ interneurons does not address whether the subgroups can originate from the same progenitor lineage at different times. To our knowledge, clonal analysis demonstrating that single radial glia can give rise to both PV- and to SST-expressing interneurons has not been published.

Within the neurochemically defined subgroups, subtypes of interneurons are defined by combinations of neurochemical, axon targeting, and electrophysiological characteristics (Wonders and Anderson 2006; Butt et al. 2007). It is possible that despite the apparent mixing of PV- and SST-expressing subgroups, distinct types of interneurons within these groups are indeed generated from highly spatially and temporally defined domains. The SST-expressing subgroup can be parsed into smaller classes that colabel with reelin, calretinin, and NPY, such that it is interesting to determine whether these subclasses have differential origins in the MGE (Gonchar et al. 2007; Miyoshi et al. 2010). Analysis of the origins of these SST^+ classes revealed that both CR and Rln coexpressing SST^+ cortical interneurons have a dorsal-high, ventral-low bias (Fig. 5), thus resembling the origins of the whole SST^+ subgroup.

Interestingly, almost none of the transplanted cells from any region of the MGE were detected to give rise to NPY^+ cells, excluding the MGE as a major source of these interneurons. In an earlier study, some NPY^+ cortical interneurons were found to derive from Nkx2.1 and/or Nkx6.2 lineage (Fogarty et al. 2007). However, both Nkx2.1 and Nkx6.2 are also expressed in the POA, which was later reported to be a source of NPY^+ cortical interneurons (Gelman et al. 2009).

In this study, the relatively small number of S-phase cells that can be labeled within a temporal window that precludes the opportunity for them to migrate extensively before transplantation limited the utility of this method for studying the mitotic origins of minor subclasses within the SST-expressing subgroups. However, our results for the origins of smaller classes within the SST^+ subgroup (Fig. 5) may also be indicative of their mitotic origins at E13.5 since the colabeling of either GFP or BrdU with SST in the transplants was highly similar at this age.

To evaluate whether an interneuron subtype may have a more discrete origin within the MGE, we took advantage of the large presence of PV-expressing interneurons in the transplants, combined with existence of a PV-expressing morphologically defined interneuron subtype and the ability to visualize the morphology of transplanted cells by immunofluorescence labeling for GFP. Relative to other MGE regions and to the E13.5 transplant, the chandelier interneurons were greatly enriched within the most ventral MGE region at E15.5 (Fig. 6). The temporal association with the later-aged transplants is consistent with the increased density of chandelier neurons, found by genetic labeling of Nkx2.1-lineage progenitors, in layer 2 of mouse neocortex (Woodruff et al. 2009). Also, since cortical interneurons derived from the more ventrally located POA primarily include NPY-expressing interneurons and not neurons with chandelier morphology (Gelman et al. 2009), this result suggests that progenitors for chandelier interneurons are enriched within the ventral-most MGE late in the period of cortical neurogenesis. This result should lead to additional gene discovery studies to determine factors associated with chandelier cell fate determination relative to that of other PV-expressing interneurons. As abnormalities of chandelier interneurons have been associated with epilepsy and schizophrenia (Ribak 1985; Freund and Buzsaki 1988; Marco et al. 1996; Arellano et al. 2004; Lewis et al. 2005), such studies could have important clinical implications.

In addition to the relevance of this work for guiding future studies of interneuron fate determination, MGE transplantation into hippocampus and neocortex has become an important tool for modifying cortical activity in vivo. To date, MGE transplants into postnatal cortex have been shown to enhance local inhibition (Alvarez-Dolado et al. 2006), alter cortical plasticity (Southwell et al. 2010), and reduce seizures in early postnatal neocortex and in adult hippocampus (Baraban et al. 2009; Waldau et al. 2010; Zipancic et al. 2010). Moreover, MGE transplants into adult striatum can reduce abnormal turning

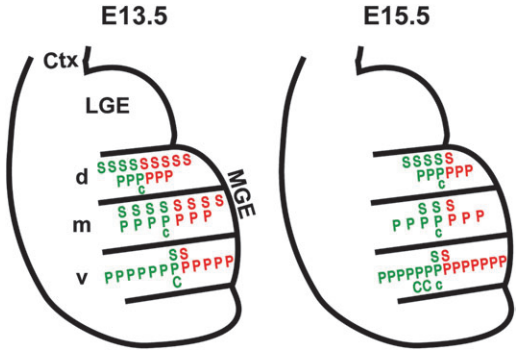

Figure 6. Summary of the spatial and temporal differences in the origins of SST^+, PV^+, and chandelier interneurons. Green indicates counts of GFP^+ neurons in the transplants, whereas red indicates counts of $BrdU^+$ cells. Capital letters indicate, approximately, each 10% of cells in the transplant expressing SST (S), parvalbumin (P), or having a chandelier interneuron morphology (C). The lower-case (c) indicates roughly 5%. Note that in general, the results from counts of GFP or BrdU-labeled cells are similar, whereas these counts are highly discordant in the case of SST^+ cells in the dMGE at E15.5. In addition, there is a remarkable enrichment for chandelier interneurons in the vMGE transplants at E15.5. (Ctx: Cortex, d: dorsal, m: middle, v: ventral).

behavior in a model of Parkinson's disease (Martinez-Cerdeno et al. 2010). Since the PV- and SST-expressing subgroups have distinct intrinsic firing properties and distinct propensities for targeting the perisomatic versus distal dendritic regions of pyramidal neurons (Markram et al. 2004; Ascoli et al. 2008), better understanding of interneuron subgroup compositions from transplants of temporally and spatially defined MGE sources informs future transplantation studies (Fig. 6).

Funding

National Institutes of Mental Health (R01 MH066912, K02 MH070031).

Notes

We would like to acknowledge Dr Tim Petros for his invaluable comments on this manuscript. *Conflict of Interest:* None declared.

References

Alvarez-Dolado M, Calcagnotto ME, Karkar KM, Southwell DG, Jones-Davis DM, Estrada RC, Rubenstein JL, Alvarez-Buylla A, Baraban SC. 2006. Cortical inhibition modified by embryonic neural precursors grafted into the postnatal brain. J Neurosci. 26:7380–7389.

Anderson SA, Marin O, Horn C, Jennings K, Rubenstein JL. 2001. Distinct cortical migrations from the medial and lateral ganglionic eminences. Development. 128:353–363.

Arellano JI, Munoz A, Ballesteros-Yanez I, Sola RG, DeFelipe J. 2004. Histopathology and reorganization of chandelier cells in the human epileptic sclerotic hippocampus. Brain. 127:45–64.

Ascoli GA, Alonso-Nanclares L, Anderson SA, Barrionuevo G, Benavides-Piccione R, Burkhalter A, Buzsaki G, Cauli B, Defelipe J, Fairen A, et al. 2008. Petilla terminology: nomenclature of features of GABAergic interneurons of the cerebral cortex. Nat Rev Neurosci. 9:557–568.

Baraban SC, Southwell DG, Estrada RC, Jones DL, Sebe JY, Alfaro-Cervello C, Garcia-Verdugo JM, Rubenstein JL, Alvarez-Buylla A. 2009. Reduction of seizures by transplantation of cortical GABAergic interneuron precursors into Kv1.1 mutant mice. Proc Natl Acad Sci U S A. 106:15472–15477.

Batista-Brito R, Fishell G. 2009. The developmental integration of cortical interneurons into a functional network. Curr Top Dev Biol. 87:81–118.

Butt SJ, Cobos I, Golden J, Kessaris N, Pachnis V, Anderson S. 2007. Transcriptional regulation of cortical interneuron development. J Neurosci. 27:11847–11850.

Cavanagh ME, Parnavelas JG. 1988. Development of somatostatin immunoreactive neurons in the rat occipital cortex: a combined immunocytochemical-autoradiographic study. J Comp Neurol. 268:1–12.

Cobos I, Calcagnotto ME, Vilaythong AJ, Thwin MT, Noebels JL, Baraban SC, Rubenstein JL. 2005. Mice lacking Dlx1 show subtype-specific loss of interneurons, reduced inhibition and epilepsy. Nat Neurosci. 8:1059–1068.

DeFelipe J. 1999. Chandelier cells and epilepsy. Brain. 122(Pt 10):1807–1822.

DeFelipe J, Hendry SH, Jones EG, Schmechel D. 1985. Variability in the terminations of GABAergic chandelier cell axons on initial segments of pyramidal cell axons in the monkey sensory-motor cortex. J Comp Neurol. 231:364–384.

Du T, Xu Q, Ocbina PJ, Anderson SA. 2008. NKX2.1 specifies cortical interneuron fate by activating Lhx6. Development. 135:1559–1567.

Fazzari P, Paternain AV, Valiente M, Pla R, Lujan R, Lloyd K, Lerma J, Marin O, Rico B. 2010. Control of cortical GABA circuitry development by Nrg1 and ErbB4 signalling. Nature. 464:1376–1380.

Flames N, Pla R, Gelman DM, Rubenstein JL, Puelles L, Marin O. 2007. Delineation of multiple subpallial progenitor domains by the combinatorial expression of transcriptional codes. J Neurosci. 27:9682–9695.

Flandin P, Kimura S, Rubenstein JL. 2010. The progenitor zone of the ventral medial ganglionic eminence requires Nkx2-1 to generate most of the globus pallidus but few neocortical interneurons. J Neurosci. 30:2812–2823.

Fogarty M, Grist M, Gelman D, Marin O, Pachnis V, Kessaris N. 2007. Spatial genetic patterning of the embryonic neuroepithelium generates GABAergic interneuron diversity in the adult cortex. J Neurosci. 27:10935–10946.

Freund TF, Buzsaki G. 1988. Alterations in excitatory and GABAergic inhibitory connections in hippocampal transplants. Neuroscience. 27:373–385.

Gelman DM, Marin O. 2010. Generation of interneuron diversity in the mouse cerebral cortex. Eur J Neurosci. 31:2136–2141.

Gelman DM, Martini FJ, Nobrega-Pereira S, Pierani A, Kessaris N, Marin O. 2009. The embryonic preoptic area is a novel source of cortical GABAergic interneurons. J Neurosci. 29:9380–9389.

Glickstein SB, Moore H, Slowinska B, Racchumi J, Suh M, Chuhma N, Ross ME. 2007. Selective cortical interneuron and GABA deficits in cyclin D2-null mice. Development. 134:4083–4093.

Gonchar Y, Wang Q, Burkhalter A. 2007. Multiple distinct subtypes of GABAergic neurons in mouse visual cortex identified by triple immunostaining. Front Neuroanat. 1:3.

Gulacsi AA, Anderson SA. 2008. Beta-catenin-mediated Wnt signaling regulates neurogenesis in the ventral telencephalon. Nat Neurosci. 11:1383–1391.

Jessell TM. 2000. Neuronal specification in the spinal cord: inductive signals and transcriptional codes. Nat Rev Genet. 1:20–29.

Lee SK, Pfaff SL. 2001. Transcriptional networks regulating neuronal identity in the developing spinal cord. Nat Neurosci. 4(Suppl):1183–1191.

Lewis DA, Hashimoto T, Volk DW. 2005. Cortical inhibitory neurons and schizophrenia. Nat Rev Neurosci. 6:312–324.

Malicki J. 2004. Cell fate decisions and patterning in the vertebrate retina: the importance of timing, asymmetry, polarity and waves. Curr Opin Neurobiol. 14:15–21.

Marco P, Sola RG, Pulido P, Alijarde MT, Sanchez A, Ramon y Cajal S, DeFelipe J. 1996. Inhibitory neurons in the human epileptogenic temporal neocortex. An immunocytochemical study. Brain. 119(Pt 4):1327–1347.

Markram H, Toledo-Rodriguez M, Wang Y, Gupta A, Silberberg G, Wu C. 2004. Interneurons of the neocortical inhibitory system. Nat Rev Neurosci. 5:793–807.

Martinez-Cerdeno V, Noctor SC, Espinosa A, Ariza J, Parker P, Orasji S, Daadi MM, Bankiewicz K, Alvarez-Buylla A, Kriegstein AR. 2010. Embryonic MGE precursor cells grafted into adult rat striatum integrate and ameliorate motor symptoms in 6-OHDA-lesioned rats. Cell Stem Cell. 6:238–250.

Miyoshi G, Butt SJ, Takebayashi H, Fishell G. 2007. Physiologically distinct temporal cohorts of cortical interneurons arise from telencephalic Olig2-expressing precursors. J Neurosci. 27:7786–7798.

Miyoshi G, Hjerling-Leffler J, Karayannis T, Sousa VH, Butt SJ, Battiste J, Johnson JE, Machold RP, Fishell G. 2010. Genetic fate mapping reveals that the caudal ganglionic eminence produces a large and diverse population of superficial cortical interneurons. J Neurosci. 30:1582–1594.

Pesold C, Impagnatiello F, Pisu MG, Uzunov DP, Costa E, Guidotti A, Caruncho HJ. 1998. Reelin is preferentially expressed in neurons synthesizing gamma-aminobutyric acid in cortex and hippocampus of adult rats. Proc Natl Acad Sci U S A. 95(6):3221–3226.

Ribak CE. 1985. Axon terminals of GABAergic chandelier cells are lost at epileptic foci. Brain Res. 326:251–260.

Rymar VV, Sadikot AF. 2007. Laminar fate of cortical GABAergic interneurons is dependent on both birthdate and phenotype. J Comp Neurol. 501:369–380.

Somogyi P. 1977. A specific 'axo-axonal' interneuron in the visual cortex of the rat. Brain Res. 136:345–350.

Somogyi P, Freund TF, Cowey A. 1982. The axo-axonic interneuron in the cerebral cortex of the rat, cat and monkey. Neuroscience. 7:2577–2607.

Sousa VH, Miyoshi G, Hjerling-Leffler J, Karayannis T, Fishell G. 2009. Characterization of Nkx6-2-derived neocortical interneuron lineages. Cereb Cortex. 19(Suppl 1):i1–10.

Southwell DG, Froemke RC, Alvarez-Buylla A, Stryker MP, Gandhi SP. 2010. Cortical plasticity induced by inhibitory neuron transplantation. Science. 327:1145–1148.
Volk DW, Lewis DA. 2002. Impaired prefrontal inhibition in schizophrenia: relevance for cognitive dysfunction. Physiol Behav. 77:501–505.
Waldau B, Hattiangady B, Kuruba R, Shetty AK. 2010. Medial ganglionic eminence-derived neural stem cell grafts ease spontaneous seizures and restore GDNF expression in a rat model of chronic temporal lobe epilepsy. Stem Cells. 28:1153–1164.
Welagen J, Anderson SA. 2011. Origins of neocortical interneurons in mice. Develop Neurobiol. 71:10–17
Wonders CP, Anderson SA. 2006. The origin and specification of cortical interneurons. Nat Rev Neurosci. 7:687–696
Wonders CP, Taylor L, Welagen J, Mbata IC, Xiang JZ, Anderson SA. 2008. A spatial bias for the origins of interneuron subgroups within the medial ganglionic eminence. Dev Biol. 314:127–136.
Woodruff A, Xu Q, Anderson SA, Yuste R. 2009. Depolarizing effect of neocortical chandelier neurons. Front Neural Circuits. 3:15.
Xu Q, Guo L, Moore H, Waclaw RR, Campbell K, Anderson SA. 2010. Sonic hedgehog signaling confers ventral telencephalic progenitors with distinct cortical interneuron fates. Neuron. 65:328–340.
Xu Q, Tam M, Anderson SA. 2008. Fate mapping Nkx2.1-lineage cells in the mouse telencephalon. J Comp Neurol. 506:16–29.
Xu X, Roby KD, Callaway EM. 2010. Immunochemical characterization of inhibitory mouse cortical neurons: three chemically distinct classes of inhibitory cells. J Comp Neurol. 518:389–404.
Yabut O, Renfro A, Niu S, Swann JW, Marín O, D'Arcangelo G. 2007. Abnormal laminar position and dendrite development of interneurons in the reeler forebrain. Brain Res. 1140:75–83.
Zipancic I, Calcagnotto ME, Piquer-Gil M, Mello LE, Alvarez-Dolado M. 2010. Transplant of GABAergic precursors restores hippocampal inhibitory function in a mouse model of seizure susceptibility. Cell Transplant. 19:549–564.